

Efficient Uncertainty Quantification in Multidisciplinary Analysis of a Reusable Launch Vehicle

Benjamin R. Bettis¹ and Serhat Hosder²

Missouri University of Science and Technology, Rolla, MO 65409

Tyler Winter³

M4 Engineering, Inc., Long Beach, California, 90807

The objective of this study was to apply a recently developed uncertainty quantification framework to the multidisciplinary analysis of a reusable launch vehicle (RLV). This particular framework is capable of efficiently propagating mixed (inherent and epistemic) uncertainties through complex simulation codes. The goal of the analysis was to quantify uncertainty in various output parameters obtained from the RLV analysis, including the maximum dynamic pressure, cross-range, range, and vehicle takeoff gross weight. Three main uncertainty sources were treated in the simulations: (1) reentry angle of attack (inherent uncertainty), (2) altitude of the initial reentry point (inherent uncertainty), and (3) the Young's Modulus (epistemic uncertainty). The Second-Order Probability Theory utilizing a stochastic response surface obtained with Point-Collocation Non-Intrusive Polynomial Chaos was used for the propagation of the mixed uncertainties. This particular methodology was applied to the RLV analysis, and the uncertainty in the output parameters of interest was obtained in terms of intervals at various probability levels. The preliminary results have shown that there is a large amount of uncertainty associated with the vehicle takeoff gross weight. Furthermore, the study has demonstrated the feasibility of the developed uncertainty quantification framework for efficient propagation of mixed uncertainties in the analysis of complex aerospace systems.

Nomenclature

C	= Mass fraction
h	= Enthalpy (J/kg)
Le	= Lewis number
n	= Number of random variables
p	= Polynomial order of total expansion
Pr	= Prandtl number
q	= Maximum dynamic pressure
R_N	= Radius of curvature (m)
α	= Reentry angle of attack
μ	= Mean
ξ	= Standard random variable
$\vec{\xi}_a$	= Standard aleatory uncertain variable vector
$\vec{\xi}_e$	= Standard epistemic uncertain variable vector
ρ	= Density (kg/m ³)
σ	= Standard deviation
σ^2	= Statistical variance
Ψ	= Random basis function

¹Graduate Student. Mechanical and Aerospace Engineering. Student Member AIAA.

²Assistant Professor of Aerospace Engineering. Mechanical and Aerospace Engineering. Senior Member AIAA.

³Aerospace Engineer, 4020 Long Beach Blvd, Long Beach, CA, 90807, Member AIAA

I. Introduction

Modeling and simulation technologies have advanced over the years with many intelligent, cost saving strategies. These technologies have assisted in the analysis and development of many complex, integrated systems. More specifically, the field of multi-disciplinary analysis and optimization (MDAO) of space systems has taken advantage of many of these technologies. Some of these technologies include design space exploration, variable-fidelity capabilities, and uncertainty and risk analysis. Furthermore, the successes of future spacecraft missions fundamentally depend on the advancement of these technologies.

The uncertainties in various parameters, operating conditions, geometry, and the physical models used in spacecraft system simulations can significantly affect the performance of the overall system. The uncertainty information obtained for the system responses can also be used in the assessment of the system robustness and/or the reliability and for decision-making in mission planning. Therefore, the quantification of uncertainties in complex integrated space systems is a key technology that warrants research and development. This challenging task requires the consideration of the propagation of various types of uncertainty (inherent and epistemic) between each subsystem and to the output quantities of interest. Several traditional uncertainty sampling methods (Monte Carlo, etc.) currently exist but have shortcomings due to their computational expense. There exists a need to be proficient in applying uncertainty methods to sophisticated systems involving high-fidelity analyses. Efficient application of uncertainty methods to these systems is crucial for providing reasonable turn-around times with computational results accompanied with various statistical metrics obtained with desired accuracy. In the current study, Second-Order Probability Theory utilizing Point-Collocation Non-Intrusive Polynomial Chaos (NIPC)¹ will be used for the propagation of mixed (aleatory-epistemic) uncertainties.²⁻³ In general, the NIPC methods, which are based on the spectral representation of uncertainty, are computationally more efficient than traditional Monte Carlo methods for moderate number of uncertain variables and can give highly accurate estimates of various uncertainty metrics. In addition, they treat the deterministic model (e.g. an RLV system) as a black box and the uncertainty information in the output is approximated with a polynomial expansion, which is constructed using a number of deterministic solutions, each corresponding to a sample point in random space. Therefore, the NIPC methods become a perfect candidate for the uncertainty quantification in the numerical solutions which are computationally expensive and complex.

Previously, M4 Engineering developed the Multidisciplinary Optimization Object Library (MOOL) as part of a phase II SBIR effort funded by NASA Glenn Research Center. An object-oriented Multidisciplinary Analysis Optimization (MDAO) framework is an automated analysis, optimization, and virtual test system that allows (1) consideration of interactions between disciplines during analysis, (2) automated execution of multiple analysis codes on different computers, (3) incorporation of test data to improve accuracy of analysis models, and (4) optimization of vehicle parameters to achieve superior performance. In the MOOL project, M4 developed a suite of common MDAO objects that can be used in multiple framework environments to handle common tasks encountered in integration of multidisciplinary analysis and optimization problems. Specifically, as an example application, a high-alpha RLV system was integrated and analyzed. In the current study, the same MOOL high-alpha RLV system will be implemented for uncertainty quantification (UQ) analysis.

M4 Engineering and Missouri S&T have partnered to develop an UQ framework. This framework is built upon an Uncertainty Module previously developed by M4 Engineering. One of the key objectives of this project is to implement the Non-Intrusive Polynomial Chaos (NIPC) expansion methods within the framework. This framework was developed in Python and primarily serves as an outer analysis layer. The utility of this framework is through the efficient application of NIPC methods to any user-specified system, which can be executed from a command line. In this paper, preliminary mixed UQ results obtained for the analysis of an RLV system are presented.

In the following section, a brief description of the various types of uncertainties found in complex numerical simulations is given. In Section III, a brief overview on the theory behind Point-Collocation

Non-Intrusive Polynomial Chaos will be given. Next in Section IV, an efficient approach to propagate mixed aleatory and epistemic uncertainties through a simulation code using NIPC and Second-Order Probability will be outlined. The uncertainty approach will first be applied to the Fay-Riddell relation for approximating stagnation point heat transfer on a blunt body (Section V). Due to the low computational costs of evaluating the Fay-Riddell relation, the results will also be compared to Monte Carlo (MC) simulation results which will assess the validity of the proposed uncertainty quantification approach. In Section VI, the MOOL RLV system will be described in detail. In Section VII, the approach for aleatory and epistemic uncertainty quantification using Point-Collocation NIPC and Second-Order Probability will be applied to the MOOL RLV system to quantify uncertainties in various performance outputs of the system. Finally in Section VIII, all relevant conclusions and future work plans will be given.

II. Types of Uncertainties in Computational Simulations

As described in Oberkampf et. al.,⁴ there can be three different types of uncertainty and error in a computational simulation: (1) aleatory uncertainty, (2) epistemic uncertainty, and (3) numerical error. The term aleatory uncertainty describes the inherent variation of a physical system. Such variation is due to the random nature of input data and can be mathematically represented by a probability density function if substantial experimental data are available for estimating the distribution (uniform, normal, etc.). The variation of the free-stream velocity or manufacturing tolerances can be given as examples for aleatory uncertainty in a stochastic external aerodynamics problem. The aleatory uncertainty is sometimes referred as irreducible uncertainty due to its nature.

Epistemic uncertainty in a non-deterministic system originates due to ignorance, lack of knowledge, or incomplete information (such as the values of transport quantities in high temperature hypersonic flow simulations). The key feature of this definition is that the fundamental cause is incomplete information of some characteristics of the system. As a result, an increase in knowledge or information can lead to a decrease in the epistemic uncertainty. Therefore, epistemic uncertainty is referred to as reducible uncertainty. As shown by Oberkampf and Helton,⁵ modeling of epistemic uncertainties with probabilistic approaches may lead to inaccurate predictions in the amount of uncertainty in the responses due to the lack of information on the characterization of uncertainty as probabilistic. One approach to characterize the epistemic uncertain variables is to use intervals. The upper and lower bounds on the uncertain variable can be prescribed using either limited experimental data or expert judgment.

Numerical error is defined as a recognizable deficiency in any phase or activity of modeling and simulation that is not due to the lack of knowledge. If errors cannot be well-characterized, then they must be treated as part of the epistemic uncertainties. The discretization error in spatial or temporal domain originating from the numerical solution of partial differential equations that describes a physical model in a discretized computational space (mesh) can be given as an example of numerical uncertainty.

III. The Point-Collocation NIPC

The polynomial chaos is a stochastic method, which is based on the spectral representation of the uncertainty. An important aspect of spectral representation of uncertainty is that one may decompose a random function (or variable) into separable deterministic and stochastic components. For example, for any random variable (i.e., α^*) in a stochastic analysis and design problem, we can write,

$$\alpha^*(\vec{x}, \vec{\xi}) = \sum_{i=0}^P \alpha_i(\vec{x}) \Psi_i(\vec{\xi}), \quad (1)$$

where $\alpha_i(\vec{x})$ is the deterministic component and $\Psi_i(\vec{\xi})$ is the random basis function corresponding to the i^{th} mode. Here we assume α^* to be a function of deterministic independent variable vector \vec{x} and the n-

dimensional random variable vector $\vec{\xi} = (\xi_1, \dots, \xi_n)$, which has a specific probability distribution. The discrete sum is taken over the number of output modes,

$$P+1 = \frac{(n+p)!}{n! p!}, \quad (2)$$

which is a function of the order of polynomial chaos (p) and the number of random dimensions (n). The basis function ideally takes the form of multi-dimensional Hermite Polynomial to span the n -dimensional random space when the input uncertainty is Gaussian (unbounded), which was first used by Wiener⁶ in his original work of polynomial chaos. Legendre (Jacobi) and Laguerre polynomials are optimal basis functions for bounded (uniform) and semi-bounded (exponential) input uncertainty distributions respectively in terms of the convergence of the statistics. Different basis functions can be used with different input uncertainty distributions (See Xiu and Karniadakis⁷ for a detailed description), however the convergence may be affected depending on the basis function used. The detailed information on polynomial chaos expansions can be found in Walters and Huyse⁸ and Hosder and Walters.¹

To model the uncertainty propagation in computational simulations via polynomial chaos with the intrusive approach, all dependent variables and random parameters in the governing equations are replaced with their polynomial chaos expansions. Taking the inner product of the equations, (or projecting each equation onto i^{th} basis) yield $P+1$ times the number of deterministic equations which can be solved by the same numerical methods applied to the original deterministic system. Although straightforward in theory, an intrusive formulation for complex problems can be relatively difficult, expensive, and time consuming to implement. To overcome such inconveniences associated with the intrusive approach, non-intrusive polynomial chaos formulations have been considered for uncertainty propagation.

The collocation based NIPC method starts with replacing the uncertain variables of interest with their polynomial expansions given by Equation 1. Then, $P+1$ vectors $(\vec{\xi}_i = \{\xi_1, \xi_2, \dots, \xi_n\}_k, k = 0, 1, 2, \dots, P)$ are chosen in random space for a given PC expansion with $P+1$ modes and the deterministic code is evaluated at these points. With the left hand side of Equation 1 known from the solutions of deterministic evaluations at the chosen random points, a linear system of equations can be obtained:

$$\begin{bmatrix} \Psi_0(\vec{\xi}_0) & \Psi_1(\vec{\xi}_0) & \dots & \Psi_p(\vec{\xi}_0) \\ \Psi_0(\vec{\xi}_1) & \Psi_1(\vec{\xi}_1) & \dots & \Psi_p(\vec{\xi}_1) \\ \vdots & \vdots & \ddots & \vdots \\ \Psi_0(\vec{\xi}_P) & \Psi_1(\vec{\xi}_P) & \dots & \Psi_p(\vec{\xi}_P) \end{bmatrix} \begin{Bmatrix} \alpha_0 \\ \alpha_1 \\ \vdots \\ \alpha_P \end{Bmatrix} = \begin{Bmatrix} \alpha^*(\vec{\xi}_0) \\ \alpha^*(\vec{\xi}_1) \\ \vdots \\ \alpha^*(\vec{\xi}_P) \end{Bmatrix} \quad (3)$$

The spectral modes (α_k) of the random variable α^* are obtained by solving the linear system of equations given above. Using these, mean (μ_{α^*}) and the variance ($\sigma_{\alpha^*}^2$) of the solution can be obtained by

$$\begin{aligned} \mu_{\alpha^*} &= \alpha_0 \\ \sigma_{\alpha^*}^2 &= \sum_{i=1}^P \alpha_i^2 \langle \Psi_i^2(\vec{\xi}) \rangle \end{aligned} \quad (4)$$

The solution of the linear problem given by Equation 3 requires $P+1$ deterministic function evaluations. If more than $P+1$ samples are chosen, then the over-determined system of equations can be solved using the Least Squares method. Hosder et al.⁹ investigated this option by increasing the number of collocation points in a systematic way through the introduction of a parameter n_p defined as

$$n_p = \frac{\text{number of samples}}{P + 1}. \quad (5)$$

In the solution of stochastic model problems with multiple uncertain variables, they have used $n_p = 1, 2, 3$, and 4 to study the effect of the number of collocation points (samples) on the accuracy of the polynomial chaos expansions. Their results showed that using a number of collocation points that is twice more than the minimum number required ($n_p=2$) gives a better approximation to the statistics at each polynomial degree. This improvement can be related to the increase of the accuracy of the polynomial coefficients due to the use of more information (collocation points) in their calculation. The results of the stochastic model problems also indicated that for problems with multiple random variables, improving the accuracy of polynomial chaos coefficients in NIPC approaches may reduce the computational expense by achieving the same accuracy level with a lower order polynomial expansion.

Besides the Point-Collocation NIPC, the developed uncertainty quantification framework is capable of utilizing the Quadrature-based NIPC methods.¹ In the current study, the Point-Collocation NIPC method was implemented for the MOOL RLV application.

IV. Mixed Aleatory-Epistemic Uncertainty Propagation

In this study, Second-Order Probability²⁻³ is utilized to propagate mixed (aleatory and epistemic) uncertainty through a multidisciplinary analysis framework. Second-Order Probability uses an inner loop and an outer sampling loop as described in Figure 1. In the outer loop, a specific value for the epistemic variable is prescribed and then passed down to the inner loop. Any traditional aleatory uncertainty method may then be used to perform aleatory uncertainty analysis in the inner loop for the specified value of the epistemic uncertain variable. The Second-Order Probability will give interval bounds for the output variable of interest at different probability levels. Each iteration of the outer loop will produce a cumulative distribution function (CDF) based on the aleatory uncertainty analysis in the inner loop. Thus, if there are 100 samples in the outer loop, then 100 different CDF curves will be generated. One major advantage of Second-Order Probability is that it is easy to separate and identify the aleatory and epistemic uncertainties. On the other hand, the two sampling loops can make this method computationally expensive especially if traditional sampling techniques, such as Monte Carlo, are used for the uncertainty propagation.

The current study utilizes an efficient approach for the propagation of mixed uncertainties using the framework based on Second-Order Probability. In this approach, the stochastic response is represented with a polynomial chaos expansion on both epistemic and aleatoric variables. In this study, Point-Collocation NIPC is used to construct the stochastic response surface although other NIPC methods (i.e., quadrature or sampling based) can be also used. The optimal basis functions are used for the aleatory variables whereas Legendre polynomials are used for the epistemic uncertain variables. It should be noted that the use of Legendre polynomials should not imply a uniform probability assignment to the epistemic variables. This choice is made due to the bounded nature of epistemic uncertain variables. Once the stochastic response surface is formed, at fixed values of epistemic uncertain variables, the stochastic response values can be evaluated for a large number of samples randomly produced based on the probability distributions of the aleatoric input uncertainties (inner loop of Second-Order Probability). This procedure will produce a single cumulative distribution function. By repeating the inner loop procedure for a large number of epistemic uncertain variables sampled from their corresponding intervals (outer loop of Second-Order Probability), a population of cumulative distribution functions can be obtained which can be used to calculate the bounds of the stochastic response at different probability levels. Due to the analytical nature (polynomial) of the stochastic response, the described procedure will be computationally efficient, especially compared to the approaches based on direct MC sampling which require a large number of deterministic simulations. The overall procedure of propagating mixed

uncertainties through a simulation is given in Figure 2. Refer to Bettis and Hosder¹⁰⁻¹¹ for more information regarding the propagation of mixed uncertainties through complex simulation codes.

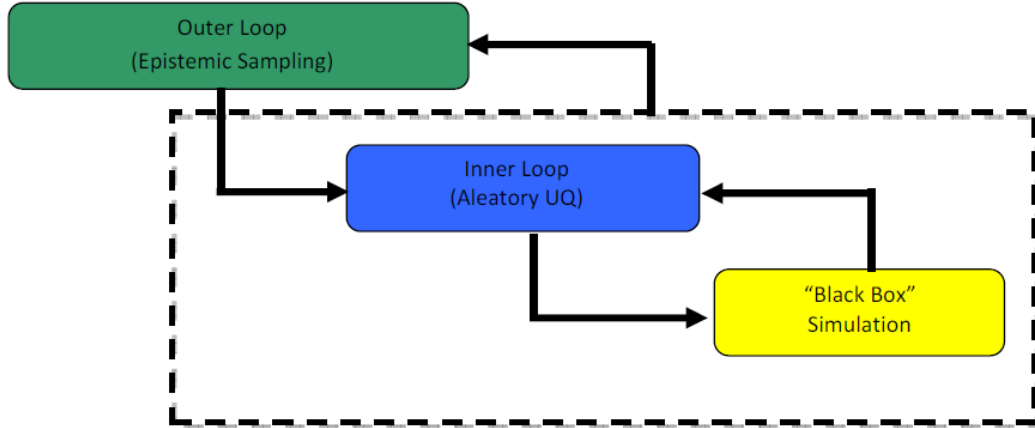


Figure 1. Schematic of second-order probability.

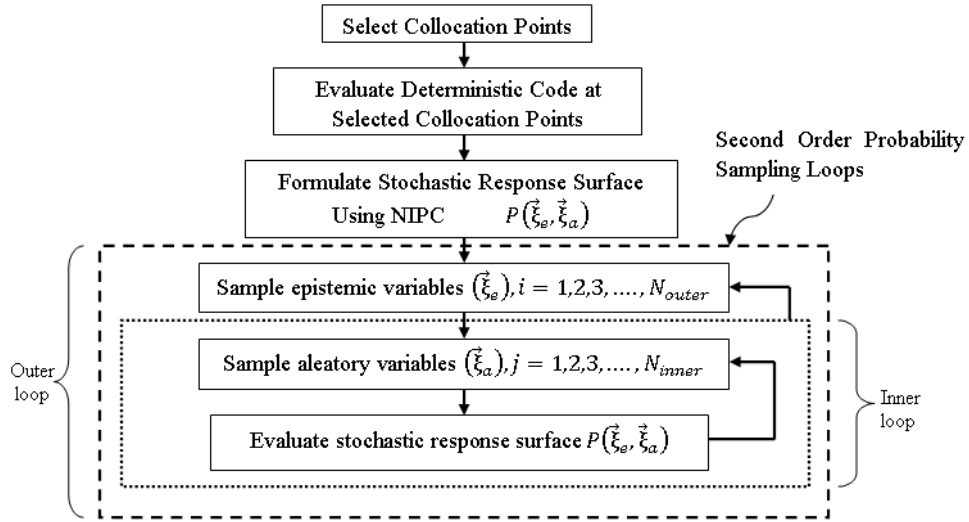


Figure 2. Flowchart describing the procedure for propagating mixed aleatory-epistemic uncertainties with Second-Order Probability and NIPC response surface.

V. Stochastic Model Problem for Stagnation Point Heat Transfer

A. Description of Deterministic Fay-Riddell Correlation

Before application to the RLV system, The mixed uncertainty quantification approach (the NIPC method and Second-Order Probability) was implemented to a model problem, which included the prediction of stagnation point heat flux on a blunt body. For this model problem, it was assumed that the boundary layer was laminar, flow was in equilibrium, and the vehicle's wall was fully catalytic. With these assumptions, an analytical correlation for the stagnation heat flux was given by Fay and Riddell.¹²

$$\dot{q}_w = 0.76(Pr_w)^{-0.6}(\rho_e \mu_e)^{0.4}(\rho_w \mu_w)^{0.1} \sqrt{\left(\frac{dU_e}{dx}\right)_{sp}} (h_{oe} - h_w) \left[1 + \left(Le^{0.63} - 1 \right) \left(\frac{h_D}{h_{oe}} \right) \right] \quad (6)$$

Where,

$$\left(\frac{dU_e}{dx}\right)_{sp} = \frac{1}{R_N} \sqrt{\frac{2(p_e - p_\infty)}{\rho_e}} \quad (7)$$

$$h_D = \gamma \sum_i C_{i_e} (\Delta h_f)^{\circ} \quad (8)$$

In Equation 6, the Pr symbolizes the Prandtl Number which was assumed to be 0.714 and Le symbolizes the Lewis Number which was taken to be 1.4. The subscripts e and w represent the property at the edge of the boundary layer and at the wall of the vehicle respectively. Also, R_N represents the radius of curvature of the blunt body. In Equation 8, C_i represents the species mass fraction behind the normal shock wave which was calculated using statistical thermodynamics. The heats of formation at absolute zero, $(\Delta h_f)^{\circ}$, were taken as zero for the molecules. The properties behind the normal shock were found with equilibrium air assumption using thermodynamic curve. The wall temperature was held constant at 300 K (cold-wall boundary condition). For more details on this model problem, please refer to Bettis and Hosder.¹⁰

B. Description of the Stochastic Problem

For this case, the free-stream velocity and the dynamic viscosity at the boundary layer edge (μ_e) were treated as random variables within the Fay-Riddell relation in Equation 6. The free-stream velocity was assumed to be an inherent uncertain variable and the coefficient of viscosity (physical model parameter) was assumed to be an epistemic uncertain variable. The dynamic viscosity was modeled using Sutherland's Law. It is known that the accuracy of Sutherland's Law degrades at high temperatures (beyond 3000 K) due to dissociation and ionization effects. One can use high-order models or curve-fits to increase the prediction accuracy of viscosity at high temperatures. However, by retaining Sutherland's law in this study, an epistemic uncertainty is intentionally introduced to the model problem. In specific, the coefficient of viscosity was modeled as an epistemic variable through the introduction of a factor (k) which is multiplied with the value obtained with Sutherland's Law (e.g., $\mu_e = k (\mu_{e,ref})$). This factor is treated as an epistemic uncertain variable with a specified interval which had the upper and lower bounds of [1.0, 1.15]. The procedure for calculating these bounds is shown in Bettis and Hosder.¹⁰

The free-stream velocity was assumed to have a uniform distribution with a mean of 4167 m/s.¹⁰ The lower and upper bounds were set at 3958.65 m/s and 4375.35 m/s respectively which correspond to a 5% uncertainty in the free-stream velocity. For comparison purposes, the free-stream velocity was also modeled as a normal random variable with a mean of 4167 m/s and a standard deviation of 100 m/s.

B. Mixed Aleatory-Epistemic Uncertainty Quantification

The approach described previously was followed to propagate the mixed (aleatory and epistemic) uncertainty through the Fay-Riddell relation. Convergence studies were carried out and it was found that a 3rd order polynomial chaos was sufficient for convergence of the NIPC response surface. A Latin Hypercube Sample (LHS) of size 5,000 was used for the outer loop (epistemic) sampling. For each value of μ , the NIPC response surface was utilized for the inner loop (aleatory) UQ, which produced a single cumulative distribution function (CDF). The overall Second-Order Probability analysis produced 5,000 CDF curves.

Figure 3 shows the mixed uncertainty results for uniformly distributed velocity and Figure I 4 displays the results for velocity modeled with a normal distribution. In each figure, the left plot shows the results

obtained with Second-Order Probability approach with the NIPC response surface formulation and the right plot gives the results obtained with a direct Monte Carlo (MC) approach that utilized 10,000 samples for the outer loop and 5,000 samples for the inner loop (a total number of 5×10^7 Fay-Riddell evaluations). By comparing the results of NIPC and MC, it can clearly be seen that the NIPC results compare well with MC. This indicates that the stochastic response surface approach to Second-Order Probability is performing well. These results provide confidence for using the same method in other expensive computational simulations. Figure 3 and Figure 4 also imply a fairly linear dependency of stagnation point heat transfer on the statistical distribution type of the free-stream velocity. In Figure 3, the velocity has a uniform distribution and the CDF shapes show that the distribution of stagnation heat transfer is fairly uniform as well. Similarly for Figure 4, the velocity has a Gaussian distribution and the CDF curves for stagnation point heat transfer are very similar to typical Gaussian CDF curves. These results also demonstrate the importance of distribution type for modeling aleatory uncertain variables. When the distribution type for the velocity was changed from uniform to normal, the results from Second-Order Probability were also significantly altered.

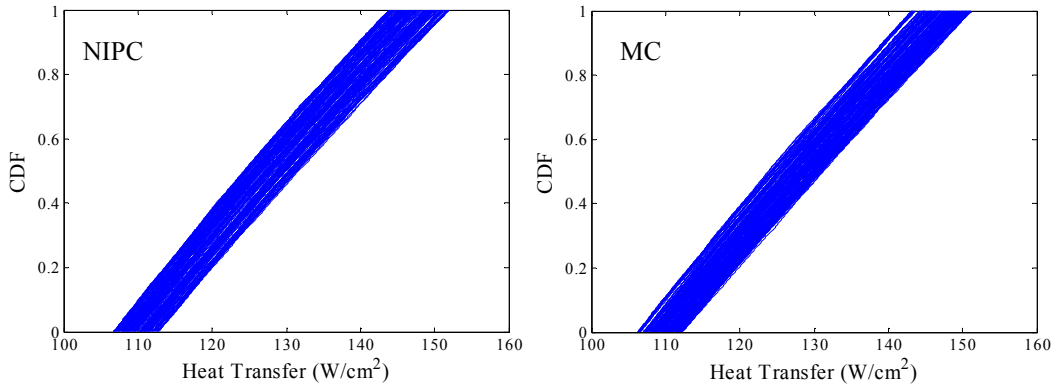


Figure 3. Horse-tail plot representing mixed aleatory-epistemic uncertainty results for the Fay-Riddell model problem (uniform distribution for velocity).

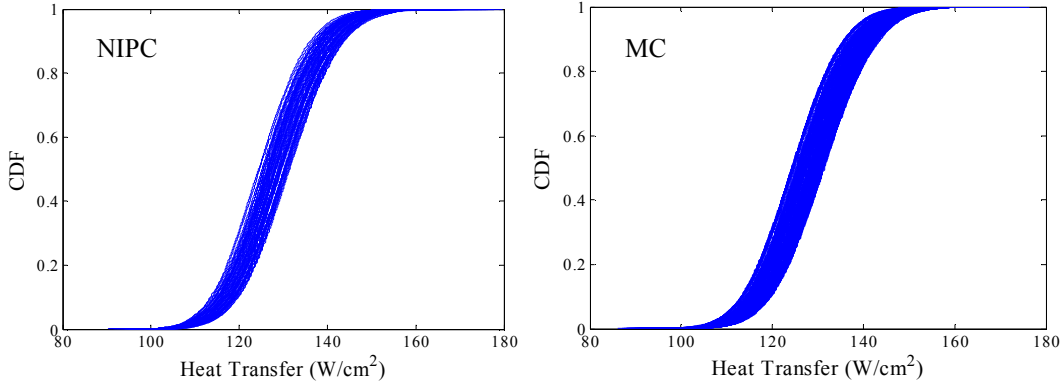


Figure 4. Horse-tail plot representing mixed aleatory-epistemic uncertainty results for the Fay-Riddell model problem (normal distribution for velocity).

Stagnation heat flux information at particular probability levels are shown in Table 1 and Table 2, which is for the uniform and normal distribution of free-stream velocity, respectively. In these tables, the heat flux uncertainty results obtained from Second-Order Probability are reported using intervals at each probability level. The second column in the table is for the results obtained with the NIPC response surface formulation for uncertainty propagation and the third column shows results obtained with the MC.

Once again, the NIPC results are consistent with the MC, which demonstrates the effectiveness of the NIPC method. The fourth column lists the results from a pure aleatory uncertainty analysis that modeled the coefficient of viscosity as a uniform random variable. The same 3rd order NIPC response surface was used to propagate the aleatory uncertainty. Although it may not be appropriate to treat the coefficient of viscosity as a probabilistic uncertainty due to its nature, the results are shown here for the purpose of comparison to mixed uncertainty results. It can be seen that only a single value is available (not an interval) at each probability level for the aleatory NIPC results.

Table 1. Stagnation point heat transfer (W/cm²) at different probability levels for the model problem (Free-stream velocity is taken as a uniform random variable).

Probability Level	Second-Order Probability (NIPC)	Second-Order Probability (MC)	Aleatory (NIPC)
P = 0.0	[106.67, 112.80]	[106.18, 112.29]	106.86
P = 0.2	[113.25, 120.36]	[112.97, 119.86]	116.92
P = 0.4	[120.23, 128.06]	[120.15, 127.45]	124.32
P = 0.6	[127.62, 135.87]	[127.48, 135.26]	131.91
P = 0.8	[135.37, 144.04]	[135.16, 143.20]	139.89
P = 1.0	[143.86, 152.13]	[143.14, 151.37]	151.94

Table 2. Stagnation point heat transfer (W/cm²) at different probability levels for the model problem (Free-stream velocity is taken as a normal random variable).

Probability Level	Second-Order Probability (NIPC)	Second-Order Probability (MC)	Aleatory (NIPC)
P = 0.0	[81.80, 103.29]	[83.31, 101.73]	90.14
P = 0.2	[116.81, 124.10]	[116.72, 123.78]	120.35
P = 0.4	[121.90, 129.45]	[121.94, 129.21]	125.67
P = 0.6	[126.42, 134.24]	[126.42, 133.91]	130.43
P = 0.8	[131.63, 139.88]	[131.76, 139.61]	136.07
P = 1.0	[154.78, 186.28]	[156.07, 184.57]	168.41

VI. MOOL Reusable Launch Vehicle System

A. Integrated Spacecraft System – RLV Demonstration Application

The MOOL RLV analysis framework application includes Modules (objects) to handle the disciplines of Geometry, Aerodynamics, Trajectory, Thermal, Structural Optimization, Mission Performance, and Optimization. These modules were implemented using off-the-shelf software in most cases, with some custom code developed as required. The configuration used in this hypersonic process is a vehicle configuration from the Air Force High Alpha RLV Aerodynamic Configuration Development Program. The purpose of the development program was to perform tests and validate the CFD codes used for predicting airflow around the six different vehicle configurations being researched. The RLV configuration used in this MDAO process is shown in Figure 5. This process is discussed in detail below. The implemented RLV process seamlessly handles the passing of data between modules. Ultimately, this allows system level optimization and trade studies to be performed.

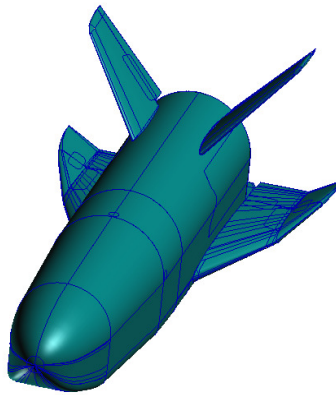


Figure 5. RLV Vehicle Configuration F.

The overall process for MDAO of the RLV is shown schematically in Figure 6. The process is shown in Design Structure Matrix format, in which the inputs to a module are shown in the same column as the module, and the outputs are shown on the same row (with the exception of the far left column, which represents overall process inputs). For example the FEM Mesh (on the same row as Geometry and the same column as Structural) is generated by the Geometry module and used by the Structural module. The modules are listed in execution order along the diagonal, starting with geometry and ending with mission performance. Only the most important interactions are shown.

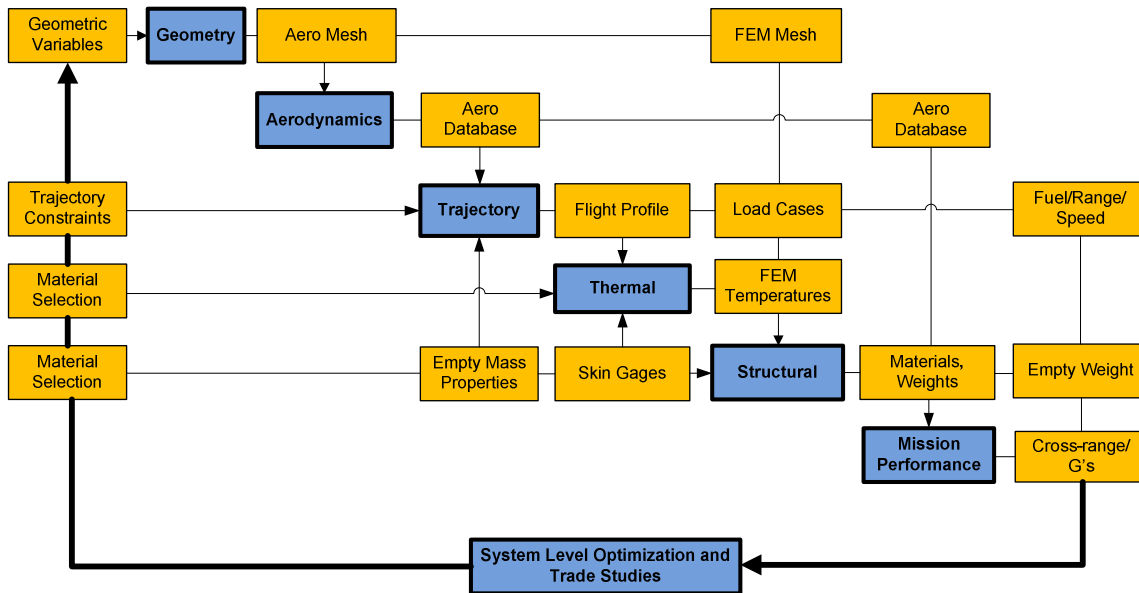


Figure 6. RLV design structure matrix.

B. Modules Included in MOOL RLV System

The following subsystem modules were incorporated into the RLV system model:

1. **Geometry** - The Geometry Module is responsible for morphing analytical meshes for use by the MOOL system.

2. **Aerodynamics** - The Aerodynamics Module is responsible for calculating aerodynamics (in the form of an aerodynamic database) for a reusable launch vehicle configuration.
3. **Trajectory** – The Trajectory Module is responsible for determining the optimum trajectory for three types of launch vehicle trajectories. These include ascent, descent, and boost/flyback.
4. **Thermal** – The Thermal Module is responsible for calculating the temperature response of all structural components subjected to aero heating and to determine the necessary material thicknesses for the thermal protection system (TPS).
5. **Structural** - The Structural Module is responsible for analyzing a user-supplied structural model and optimizing the structural sizing to minimize the structural weight.
6. **Mission Performance** - The Mission Module provides the system-level integration of the results from the steady aerodynamics, propulsion/power, and structural optimization modules to evaluate the overall performance of the vehicle.
7. **Optimization** – The Optimization Module is responsible for building tools for sample point generation by using Design of Experiments (DOE), creating metamodels (surrogate models) for multi-fidelity correction functions, and performing design optimization.

The MOOL RLV system serves to provide system-level performance analysis of a particular RLV design configuration. System-level design and optimization can be carried out fairly effortlessly using this analysis framework.

VII. Uncertainty Quantification for the MOOL Reusable Launch Vehicle System

A. Description of the Stochastic Problem

The MOOL RLV system has a large number of input parameters. Many of these parameters are propagated through multiple subsystem modules and can have a significant impact on the overall output of the system. Uncertainties (inherent and epistemic) can also be associated with some of the input parameters which can greatly affect the output of the MOOL RLV system analysis. For the demonstration problem of applying the efficient uncertainty quantification techniques to an integrated aerospace system, three input uncertainties selected. Two inherent (aleatory) parameters and one epistemic (model form) uncertainty were chosen. The altitude of the initial re-entry point was selected as one inherent uncertainty. The re-entry altitude, which can be thought of as an initial condition, was selected as an uncertainty source because a small deviation from the nominal altitude can greatly affect the overall trajectory of the re-entry vehicle which also gets propagated through many of the subsystem modules. The altitude was assumed to have a normal distribution with a mean of 295,000 feet and a standard deviation of 1,666.67 feet. The second inherent uncertainty selected was the re-entry angle of attack (α). The parameter α was assumed to have a normal distribution with a mean of 60° and a standard deviation of 1.667° . The third uncertain parameter was chosen to be the Young's Modulus. The RLV system is a futuristic concept vehicle, and so there is some level of uncertainty in the technological advances in structural materials which will be used to construct these types of vehicles. Therefore, the structural property, Young's Modulus, was treated as an epistemic uncertainty to account for the unknown material that will be used in future manufacturing of the RLV. The lower and upper bounds for the Young's Modulus was selected as 25,000,000 psi and 29,600,000 psi, respectively. An overview of the input uncertainties is shown in Table 3.

The mixed uncertainties were propagated through the MOOL RLV system to a total of four output variables which are of interest in the design of a RLV system. The four output variables analyzed were the maximum range, maximum cross range, maximum dynamic pressure (q), and the takeoff gross weight (TOGW).

Table 3. Uncertainty ranges for the parameters used in the RLV problem.

Uncertain Parameter	Uncertainty Type	Uncertainty Range
Altitude	Aleatory (normal)	$\mu = 295,000 \text{ ft}, \sigma = 1,666.67 \text{ ft}$
α	Aleatory (normal)	$\mu = 60^\circ, \sigma = 1.6667^\circ$
Young's Modulus	Epistemic	[25,000,000 psi, 29,600,000 psi]

B. Mixed Uncertainty Quantification for the RLV Application

The approach described previously was followed to propagate the mixed (aleatory and epistemic) uncertainty through the RLV application problem. For this particular case, Point-Collocation NIPC with an oversampling ratio of two was utilized to formulate the response surface which was implemented into the sampling loops of Second-Order Probability. Convergence studies were carried out and it was found that a 4th order polynomial chaos was sufficient for convergence of the NIPC response surface. This required a total of 70 MOOL RLV system evaluations (Equation 2). A Latin Hypercube Sample (LHS) of size 1,000 was used for the outer loop (epistemic) sampling. For each iteration of the outer loop in Second-Order Probability, the NIPC response surface was utilized for the inner loop (aleatory) UQ, with 1,000 samples, which produced a single cumulative distribution function (CDF). The overall Second-Order Probability analysis produced 1,000 CDF curves, which were then evaluated to find the upper and the lower bounds of the output variables of interest at various probability levels.

The interval bounds at various probability levels for each of the four output variables of interest (maximum range, maximum cross range, maximum dynamic pressure, and TOGW) are shown in Table 4. The interval range for maximum range, maximum cross range, and maximum dynamic pressure (q) are much smaller compared to the interval range of TOGW. This result implies that the epistemic uncertainty (Young's Modulus) has the largest impact on TOGW. However, the maximum range, maximum cross range, and maximum dynamic pressure have a significant amount of uncertainty due to the aleatory (inherent) input uncertainties. There is a relatively large interval range for TOGW at all probability levels. This result directly implies that the Young's Modulus (epistemic uncertainty) has a significant contribution to the uncertainty in the vehicle's TOGW. Uncertainty in TOGW is important from a design point of view because a vehicle's takeoff weight directly affects the vehicle's capacity for carrying payload, fuel, etc.

Table 4. Interval bounds for the output variables of interest at various probability levels.

Probability Level	Maximum Range (miles)	Maximum Cross Range (miles)	Maximum q (psf)	Maximum TOGW (lbs)
P = 0.05	[985.33, 987.65]	[1158.36, 1160.52]	[126.19, 146.59]	[26304.16, 28421.77]
P = 0.2	[988.17, 988.82]	[1163.20, 1164.10]	[174.83, 177.30]	[27727.63, 29523.33]
P = 0.4	[989.15, 990.17]	[1163.91, 1164.33]	[194.67, 195.97]	[28045.59, 29915.57]
P = 0.6	[989.91, 991.26]	[1164.34, 1164.64]	[206.68, 207.97]	[28270.58, 30287.93]
P = 0.8	[990.92, 992.00]	[1164.57, 1165.47]	[215.50, 217.97]	[28639.11, 30600.30]
P = 0.95	[994.74, 995.35]	[1164.80, 1166.65]	[224.13, 234.68]	[30271.89, 33030.52]

The results of the mixed (aleatory-epistemic) uncertainty quantification can be used in the assessment of the robustness or the reliability of a given vehicle. For example, in a robust design study where aleatory and epistemic uncertainties are present, one possible approach would be to minimize the variation (interval) at the mean probability level (p=50%). By shrinking this interval, the design sensitivity due to

the epistemic uncertainties would be reduced. One method for reducing the interval is by gaining a better fundamental understanding of the physics associated with the epistemic uncertainty, and developing more accurate physical models. Alternatively, the designs that are robust to the uncertainty in physical models can be developed. In a reliability-based assessment, a large interval (high epistemic uncertainty) at a specified probability level may indicate a larger design failure region for a given vehicle configuration and flight condition, which has to be addressed again with a stochastic design framework.

The demonstration problem shown here has successfully displayed the efficiency of the developed uncertainty quantification methods. In the current problem, all relevant results were obtained with 70 evaluations of the MOOL RLV system. If traditional and existing second-order probability methods were used to achieve these same results, it would require a total of 10^6 MOOL RLV system evaluations. A conservative estimate of the runtime of one MOOL RLV evaluation is approximately five hours on a single laptop PC with an Intel Core 2 Duo (2.54GHz) processor. Using this estimate, the current method of second-order probability with the NIPC response surface implementation took approximately 15 days to complete. If the traditional/existing methods were used then it would take approximately 570 years to complete all the simulations on the same computer. This relative comparison shows that the time requirement for propagating mixed uncertainties using the traditional methods is obviously not feasible for complex systems. However, the second-order probability with the NIPC response surface formulation makes it feasible to propagate mixed uncertainties in a relatively reasonable amount of time.

VIII. Conclusions

The objective of this study was to apply an efficient uncertainty quantification framework developed, which is capable of propagating mixed (aleatory and epistemic) uncertainties through complex simulation codes, to an integrated spacecraft system. In particular, the integrated spacecraft system was the MOOL Reusable Launch Vehicle (RLV) system. This particular system has multiple modules (objects) which work together to perform system level analysis for the RLV system. The developed uncertainty quantification framework was utilized to quantify the uncertainty in the RLV takeoff gross weight, cross-range, range, and maximum dynamic pressure due to epistemic and aleatory uncertainties that may exist in various parameters used in the simulation of the RLV system. For this particular study, the reentry altitude, reentry angle of attack, and the Young's Modulus were treated as uncertainties. The reentry altitude and angle of attack were treated as aleatory uncertainties described with a normal probability distribution. The Young's Modulus was modeled as an epistemic uncertain parameter and represented by using an interval. For the quantification of mixed (aleatory-epistemic) uncertainty, Second-Order Probability Theory that utilized a stochastic response surface obtained with Point-Collocation Non-Intrusive Polynomial Chaos (NIPC) Method was used.

For the stochastic MOOL RLV application problem, the mixed uncertainty quantification approach was utilized with a 4th degree stochastic response surface obtained using the Point-Collocation NIPC method with an oversampling ratio of two. This required a total of 70 MOOL RLV system executions. The uncertainty in the various output parameters was obtained in terms of intervals at different probability levels. These preliminary results indicate a relatively large amount of uncertainty in the output parameters. Future work will include comparing the Point-Collocation NIPC results with quadrature-based NIPC analysis. Furthermore, sensitivity analysis will be performed using Sobol Indices in order to achieve a relative ranking of the importance of each input uncertainty to the overall uncertainty in the output variables of interest.

Overall, the results obtained in this study show the potential of the uncertainty quantification approach that utilizes Second-Order Probability and the Non-Intrusive Polynomial Chaos for efficient and effective propagation of mixed (aleatory and epistemic) uncertainties in integrated aerospace systems.

IX. Acknowledgments

Funding for the development of the UQ Framework is provided by NASA Jet Propulsion Laboratory, STTR Project, Contract # NNX10CF64P.

X. References

¹Hosder, S. and Walters, R., "Non-Intrusive Polynomial Chaos Methods for Uncertainty Quantification in Fluid Dynamics," AIAA-Paper 2010- 0129, 48th AIAA Aerospace Sciences Meeting , Orlando, FL, January 4-7, 2010.

²Eldred, M., Swiler, L., "Efficient Algorithms for Mixed Aleatory-Epistemic Uncertainty Quantification with Application to Radiation-Hardened Electronics," Sandia National Laboratories Report, SAND2009-5805, September, 2009.

³Swiler, L., Paez, T., Mayes, R., Eldred, M., "Epistemic Uncertainty in the Calculation of Margins," AIAA-Paper 2009-2249, 50th AIAA/ASME/ASCE/AHS/ASC Structures, Structural Dynamics, and Materials Conference, Palm Springs, CA, May 4-7, 2009.

⁴Oberkampf, W. L., Helton, J. C., and Sdentz, K., "Mathematical Representation of Uncertainty, AIAA-Paper 2001-1645," 3rd Non-Deterministic Approaches Forum, Seattle, WA, April, 2001.

⁵Oberkampf, W. L. and Helton, J. C., "Investigation of Evidence Theory for Engineering Applications, AIAA-Paper 2002-1569," 4th Non-Deterministic Approaches Forum, Denver, CO, April, 2002.

⁶Wiener, N., *The Homogeneous Chaos*, American Journal of Mathematics, Vol. 60, No. 4, 1938, pp. 897–936.

⁷Xiu, D. and Karniadakis, G. E., *Modeling Uncertainty in Flow Simulations via Generalized Polynomial Chaos*, Journal of Computational Physics, Vol. 187, No. 1, May 2003, pp. 137–167.

⁸Walters, R. W. and Huyse, L., *Uncertainty Analysis for Fluid Mechanics with Applications*, T. rep., ICASE 2002-1, NASA/CR-2002-211449, NASA Langley Research Center, Hampton, VA, 2002.

⁹Hosder, S., Walters, R., and Balch, M., *Efficient Sampling for Non-Intrusive Polynomial Chaos Applications with Multiple Uncertain Input Variables*, AIAA-Paper 2007-1939, 9th AIAA Non-Deterministic Approaches Conference, Honolulu, HI, April 2007, CD-ROM.

¹⁰Bettis, B., Hosder, S., "Quantification of Uncertainty in Aerodynamic Heating of a Reentry Vehicle due to Uncertain Wall and Freestream Conditions," AIAA Paper 2010-4642, 10th AIAA/ASME Joint Thermophysics and Heat Transfer Conference, June 2010, Chicago, IL.

¹¹Bettis, B., Hosder, S., "Uncertainty Quantification in Hypersonic Reentry Flows Due to Aleatory and Epistemic Uncertainties," AIAA Paper 2011-252, 49th AIAA Aerospace Sciences Meeting, January 2011, Orlando, FL.

¹²Fay, J. A. and Riddell, F. R., "Theory of stagnation point heat transfer in dissociated air," Journal of Aeronautical Sciences, Vol. 25, No. 25, February, 1958, pp. 73-85.

¹³Ghanem, R. G., Spanos, P. D., *Stochastic Finite Elements: A spectral Approach*, Springer-Verlag, New York, 1991.